Extended-Spectrum β-Lactamase Genes Traverse the *Escherichia coli* Populations of Intensive Care Unit Patients, Staff, and Environment

Moran, Robert A; Baomo, Liu; Doughty, Emma L; Guo, Yingyi; Ba, Xiaoliang; van Schaik, Willem; Zhuo, Chao; McNally, Alan

Link to publication on Research at Birmingham portal

Extended-Spectrum β-Lactamase Genes Traverse the *Escherichia coli* Populations of Intensive Care Unit Patients, Staff, and Environment

Robert A. Moran,[a] Liu Baomo,[b*] Emma L. Doughty,[a] Yingyi Guo,[b] ⓘ Xiaoliang Ba,[c] Willem van Schaik,[a] Chao Zhuo,[b] ⓘ Alan McNally[a]

[a]Institute of Microbiology and Infection, College of Medical and Dental Sciences, University of Birmingham, Birmingham, United Kingdom
[b]State Key Laboratory of Respiratory Disease, First Affiliated Hospital of Guangzhou Medical University, Guangzhou, China
[c]Department of Veterinary Medicine, University of Cambridge, Cambridge, United Kingdom

Liu Baomo and Emma L. Doughty contributed equally to this article.

ABSTRACT Over a 3-month period, we monitored the population of extended-spectrum β-lactam-resistant *Escherichia coli* (ESBL-EC) associated with the patients, staff, and environment of an intensive care unit (ICU) in Guangzhou, China. Thirty-four clinical isolates were obtained from the same hospital 12 months later. A total of 165 isolates were characterized and whole-genome sequenced, with 24 isolates subjected to long-read sequencing. The diverse population included representatives of 59 different sequence types (STs). ICU patient and environmental isolates were largely distinct from staff isolates and clinical isolates. We observed five instances of highly similar isolates (0 to 13 single nucleotide polymorphisms [SNPs]) being obtained from different patients or bed unit environments. ESBL resistance in this collection was largely conferred by bla_{CTX-M} genes, which were found in 96.4% of all isolates. The contexts of bla_{CTX-M} genes were diverse, situated in multiple chromosomal positions and in various plasmids. We identified bla_{CTX-M}-bearing plasmid lineages that were present in multiple STs across the surveillance, staff, and clinical collections. Closer examination of IS*Ecp1*-bla_{CTX-M} transposition units shed light on the dynamics of their transmission, with evidence for the acquisition of chromosomal copies of bla_{CTX-M} genes from specific plasmid lineages and for the movement of $bla_{CTX-M-55}$ from a ST1193 chromosome to a small mobilizable plasmid. A carbapenem-resistant ST167 strain isolated from a patient that had been treated with meropenem and piperacillin-tazobactam contained seven copies of $bla_{CMY-146}$, which appears to have been amplified by IS*1*. Our data revealed limited persistence and movement of ESBL-EC strains in the ICU environment, but we observed circulating plasmid lineages playing an essential and ongoing role in shaping the cephalosporin-resistance landscape in the population examined.

IMPORTANCE ESBL resistance significantly impacts clinical management of *E. coli* infections in hospitals globally. It is important to understand the structures of ESBL-EC populations carried by hospital patients and staff, their capacity to persist in hospital environments, and the dynamics of mobile genes that drive the spread of ESBL resistance. In our 3-month study, ESBL-EC strains found in the ICU environment were strongly associated with patient carriage but distinct from strains found in staff. However, plasmid lineages carrying bla_{CTX-M} genes were found across the ICU populations and in a collection of clinical isolates obtained 1 year later. By examining their content and contexts, we have traced the recent histories of chromosomal and plasmid-borne IS*Ecp1*-bla_{CTX-M} transposition units in the ICU population. This information allowed us to implicate specific plasmid lineages in the acquisition of chromosomal bla_{CTX-M} genes, even when the plasmids were no longer present, and to detect recent transposition of $bla_{CTX-M-55}$ from a chromosome to a mobilizable plasmid.

Similar high-resolution approaches to the study of mobile genetic elements will be essential if the transmission routes associated with the spread of ESBL resistance are to be understood and subjected to interventions.

*E*scherichia coli occupies a niche in the human gastrointestinal tract that makes it an important vehicle for mobile genes that confer resistance to clinically relevant antibiotics. Some clones from the vastly diverse *E. coli* population can cause human infections (1), so the importance of antibiotic resistance gene carriage by the species is twofold, infections caused by antibiotic-resistant *E. coli* are more difficult to treat and antibiotic resistance genes carried by human-associated *E. coli* can be transferred to other Gram-negative pathogens. Extended-spectrum β-lactam (ESBL)-resistant *E. coli* (ESBL-EC) usually carry one or more of the various horizontally acquired β-lactamase (*bla*) genes that can be located in various chromosomal positions or in plasmids. The bla_{CTX-M} genes are some of the most clinically important and have been detected globally in *E. coli* and other members of the order *Enterobacterales* (2). In China, $bla_{CTX-M-55}$ has been increasing in prevalence, and in recent years, it has overtaken $bla_{CTX-M-14}$ and $bla_{CTX-M-15}$ as the most common ESBL resistance gene seen in ESBL-EC associated with human infections (3, 4).

Dissemination of ESBL resistance genes through global bacterial populations has been facilitated by mobile genetic elements (MGEs) (5). Plasmid-mediated intercellular transfer plays an obvious role in the horizontal spread of *bla* genes, but the contribution of intracellular transposition is often uncharacterized in population-level studies. The movement of *bla* genes from chromosomal sites to plasmids, or between plasmids, can increase their intercellular transfer potential. Alternatively, transposition from plasmids into chromosomal sites might increase the stability of *bla* genes in new hosts. The insertion sequence IS*Ecp1* is a major driver of intracellular bla_{CTX-M} mobility (5, 6). IS*Ecp1* can mobilize adjacent DNA by recognizing alternatives to its right inverted repeat sequence and generating transposition units (TPUs) of various sizes (5). Because TPUs can carry sequences from adjacent to their previous insertion site, in some cases it is possible to deduce their recent histories by examining their content.

It is important to understand the diversity and transmission dynamics of both ESBL-EC and *bla* gene-associated MGEs in hospital settings, particularly in intensive care units (ICUs) that host the most vulnerable patients. Although colonization by antibiotic-resistant *E. coli* has been described as a significant risk for infection in hospitals (7), genomic surveillance studies have rarely included ESBL-EC isolates that are not derived from clinical specimens (8). Genomic characterization of ESBL-EC carried asymptomatically by patients or present in hospital environments might provide insights into the dissemination of ESBL resistance. A recent genomic surveillance study of *Klebsiella pneumoniae* in a Chinese ICU highlighted the utility of considering environmental isolates when assessing hospital populations (9).

Here, we have performed a prospective observational study to examine the ESBL-EC population of an ICU in Guangzhou, China. By sampling the entire ICU patient cohort and the ICU environment weekly and by collecting rectal swabs from ICU staff, we have captured a 3-month snapshot of ESBL-EC and ESBL-resistance determinants and their associated MGEs. This information allowed us to assess the impact of *E. coli* and MGE transmission on the spread and persistence of ESBL resistance in this setting.

RESULTS

The intensive care unit hosts a diverse *E. coli* population. Over a 3-month period in 2019, 299 samples were collected from ICU patients (59 ESBL-EC positive, 19.7%), 82 from ICU staff (38 ESBL-EC positive, 46.3%), and 2,967 from the ICU environment (110 ESBL-EC positive, 3.7%). A total of 131 ESBL-EC isolates were sequenced (Fig. 1; see Table S5 in the supplemental material). Sequenced ICU surveillance isolates were derived from patient oral swabs (10 isolates) and rectal swabs (38 isolates), the ICU environment (47 isolates), and from staff rectal swabs (36 isolates). Sinks were the most common sources of
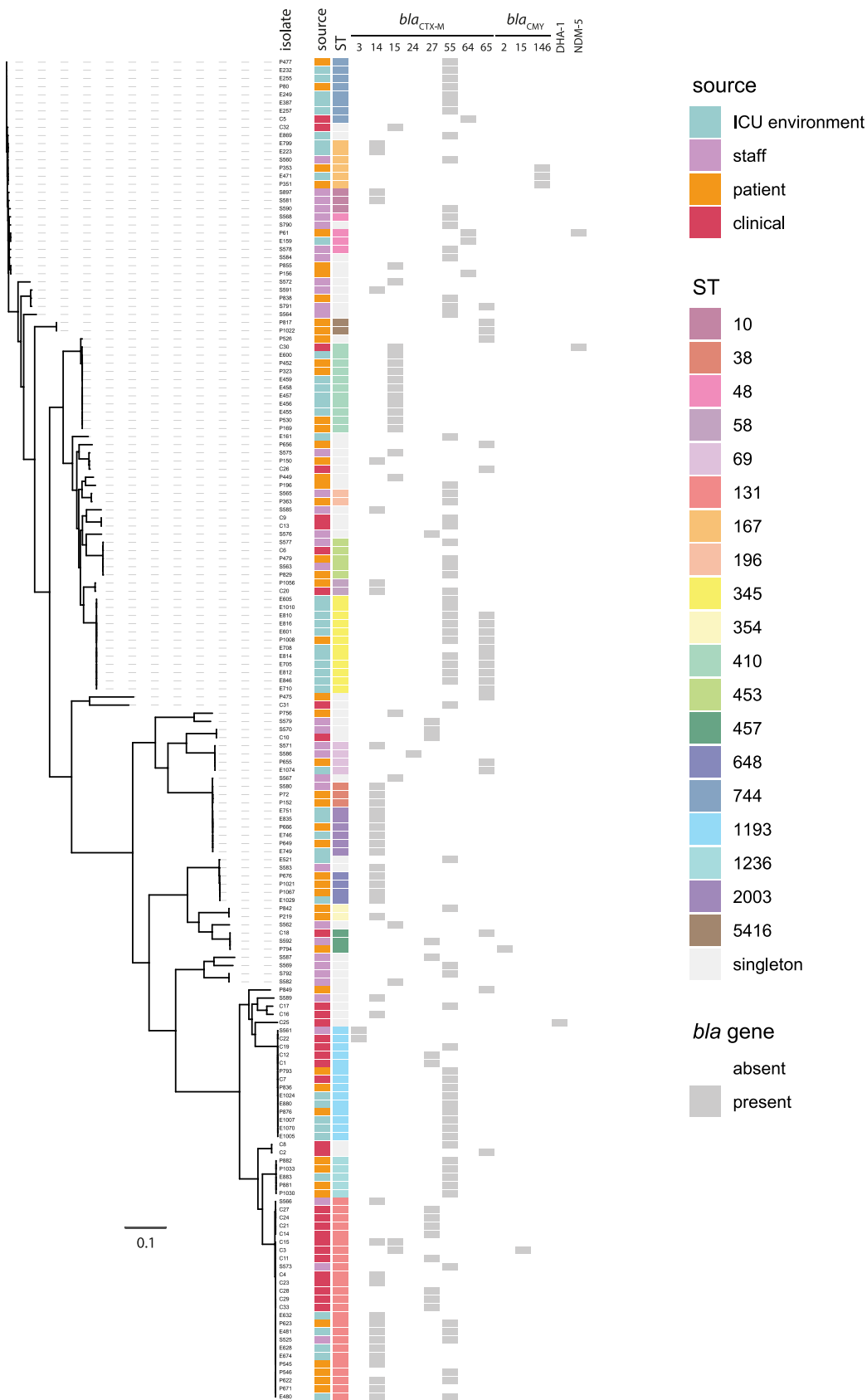
FIG 1 Maximum-likelihood phylogeny of the ESBL-EC collection assembled in this study. Isolate names are labeled to the right of dashed lines that indicate their positions in the phylogeny. To the right of the phylogeny, sources of isolation, sequence type (ST) designations, and the presence or absence of *bla* genes are indicated by colors as outlined in the key.

environmental isolates (32 of 47 isolates, 68.1%), which were obtained from sink counter-tops (12 isolates), overflows (9 isolates), drains (8 isolates), taps (2 isolates), or water (1 isolate). The remaining environmental isolates were found on bed units or equipment surfaces, including those of bed remotes (5 isolates) and bed curtains (1 isolate), a locker (1 isolate), ventilators (2 isolates), a nebulizer (1 isolate), and drip stands (2 isolates). One isolate was collected from a door handle, one from a cleaning cart, and one from a doctor's coat. A further 34 ESBL-EC isolates were obtained from clinical samples taken from patients throughout the hospital over a 2-month period in 2020.

Multilocus sequence typing revealed 50 different sequence types (STs) in the ICU surveillance collection (131 isolates) and 17 in the clinical collection (34 isolates). One ICU surveillance isolate and one clinical isolate were novel types, which were submitted to Enterobase and assigned ST12546 and ST12742. Of the 59 STs in the entire collection, 36 were represented only by single isolates and 19 were represented by between two and eight isolates. The most prevalent STs in the collection were ST131 (25 isolates), ST1193 (14), ST345 (11), and ST410 (11). Eight of the 17 STs in the clinical collection were also present in the ICU surveillance collection, namely, ST131, ST1193, ST410, ST744, ST453, ST58, ST393, and ST457.

**Environmental ESBL-EC isolates were strongly associated with patient carriage.** Visualizing the distribution of ESBL-EC isolates revealed patterns of ST, patient, and environmental associations in the ICU (Fig. 2). ESBL-EC was isolated from a patient or their bed unit on 60 sampling occasions that involved 30 different patients. On 32 of these occasions, isolates were derived from only the patient; on 15 occasions they were from only the environment; and on 13 occasions they were from both the patient and their bed unit environment. On 9 of the 13 occasions when ESBL-EC was isolated from both the patient and their bed unit environment, the environmental and patient isolates were the same ST. Of the 15 occasions on which ESBL-EC was isolated from a bed unit environment but not its resident patient, in nine the ST of the environmental isolate was the same as that of isolates that had been collected from that patient in the week(s) prior. Thus, of 60 sampling occasions where ESBL-EC was isolated from occupied bed units, 50 occasions (83.3%) involved STs obtained directly from occupying patients at the time of sampling or on previous sampling occasions.

In all 11 cases where a patient and their bed unit were sampled longitudinally, at least one ST was isolated from patient or bed unit on multiple sampling occasions. ESBL-EC isolates associated with a patient and their bed unit were usually a single ST throughout the patient's ICU stay. Only five patients (P3, P8, P16, P23, and P24) were associated with carriage of multiple STs, with those different STs isolated on separate sampling occasions (Fig. 2A). Two patients (P1 and P8) moved between bed units during the study and yielded ESBL-EC from oral or rectal swabs in both locations. In both cases, the same ST was isolated in both locations (Fig. 2A).

Evidence for strain persistence and dissemination in ICU environments. Across the ICU surveillance and clinical collections, 19 STs were associated with multiple environments, patients, or staff members. To determine whether isolates of the same ST were closely related and might be derived from a single introduction to the ICU, we evaluated whole-genome single nucleotide polymorphism (SNP) distances as well as plasmid replicon and antibiotic resistance gene content. Where available, complete genome sequences were also compared to confirm the relationships between closely related isolates. Distances between isolates of the same ST ranged from 0 to 20,795 SNPs (median, 311 SNPs; IQR, 114 to 4,536 SNPs) (see Table S6 in the supplemental material). The median maximum SNP distance between isolates of the same ST associated with a single patient was 3 SNPs (IQR, 1 to 9 SNPs), although up to 99 SNPs were found between ST345 isolates associated with P8 (see Table S7 in the supplemental material). Cases where closely related isolates of the same ST were present in multiple bed units are outlined below.

ST744 isolates were obtained from adjacent bed units 10, 11, and 12 between weeks 1 and 4 (Fig. 2). ST744 first appeared in BU11 in week 1 and was isolated from a P3 rectal swab. It was then isolated from the BU11 environment in weeks 2 and 3 before it was isolated from another P3 rectal swab in week 4. Isolates from P3 and BU11 differed by a

A Patient isolates
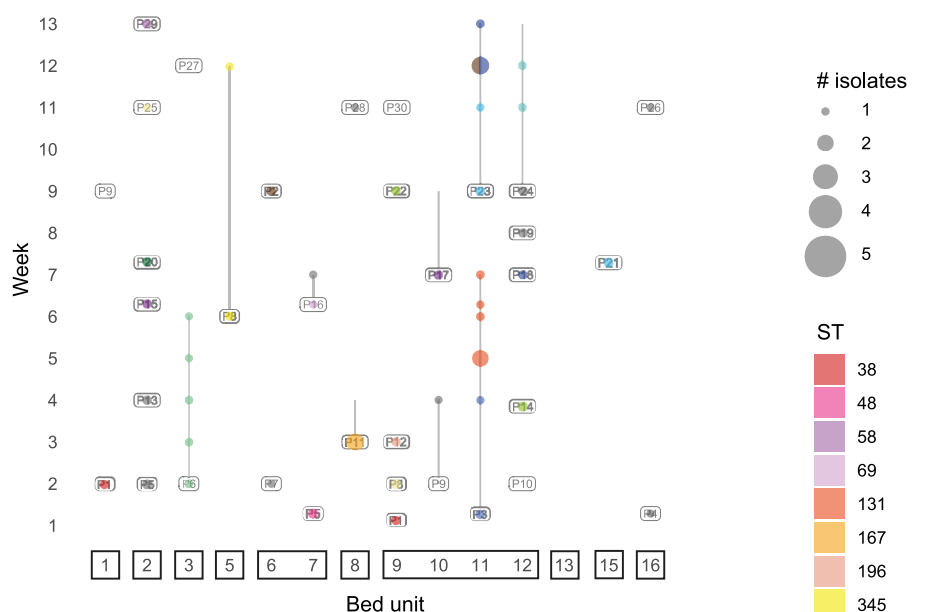
B Environmental isolates
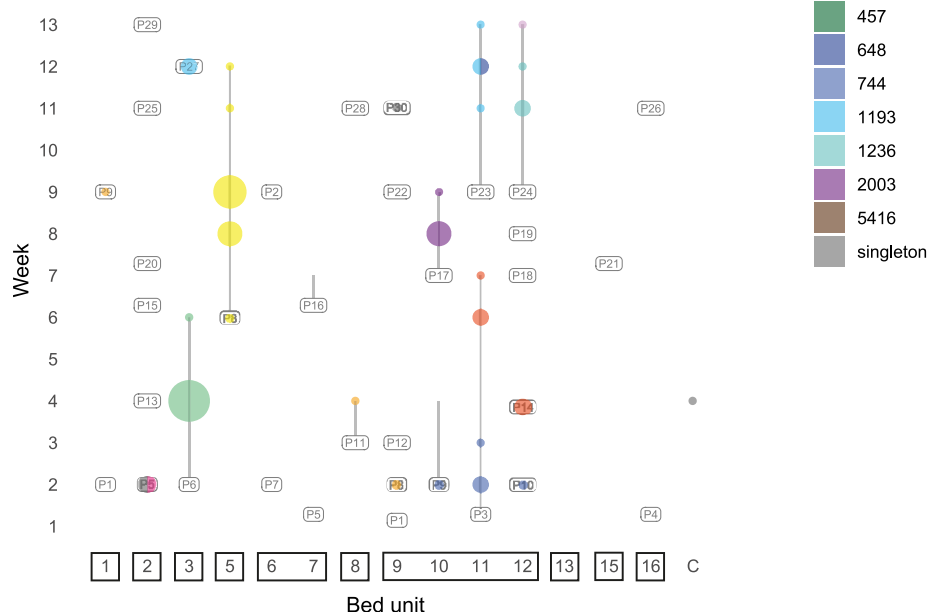
FIG 2 Distribution of ESBL-EC STs in the ICU surveillance study. Bubble plots show the distributions of patient-derived (A) and ICU environment-derived (B) ESBL-EC isolates over the course of the ICU surveillance study. The locations in which STs were isolated are indicated by colored bubbles, with the sizes of bubbles indicative of the number of isolates obtained. C, common areas outside bed units.

maximum of 3 SNPs. In week 2, ST744 isolates were also obtained from the environments of BU10 and BU12, which are in the same room as BU11 (Fig. 2B). The BU10 and BU12 isolates differed from the BU11 isolates by 1 to 2 SNPs and 9 to 13 SNPs, respectively. All ST744 isolates carried the same ARGs and plasmid replicons.

The ST744 strain in P3 appears to have been displaced by a ST131 strain over the time P3 spent in the ICU. From week 5 until their discharge from the ICU after sampling in week 7, P3 yielded ST131 isolates from oral and rectal swabs (Fig. 2A). ST131 isolates

were also obtained from the BU11 environment in weeks 6 and 7 (Fig. 2B). The P3 ST131 isolates differed by 1 to 8 SNPs from two isolates obtained from equipment in the adjacent BU12 a week earlier. Complete genomes were obtained for DETEC-E480 (BU12 environment, week 4) and DETEC-P622 (P3 rectal swab, week 6). Both genomes contain six plasmids, of which five are identical (see Fig. S1 in the supplemental material). The sixth plasmid in each genome is a FII-33:N cointegrate that differs in size and antibiotic resistance gene content due to an IS*26*-mediated deletion (Fig. S1). One ST131 isolate obtained from P3 in week 5 and all ST131 isolates from P3 or BU11 after week 6 did not contain FII-33 or N replicons or their associated resistance genes, suggesting that this plasmid had been lost. A further ST131 isolate that differed from those in P3/BU11 by 0 to 8 SNPs and contained the FII-33:N plasmid was isolated from a doctor's coat in week 8.

After P3 had been discharged, P23 occupied BU11 from week 9 to the end of the study in week 13. Over this period, 11 ST1193 isolates (0 to 8 SNPs) were collected from P23 and the BU11 environment, including from the sink. In week 12, two ST1193 isolates were obtained from the sink in BU3 (Fig. 2B). The BU3 sink isolates differed from the P23/BU11 ST1193 isolates by 0 to 7 SNPs, and all BU11/BU3 isolates carried the same antibiotic resistance genes (ARGs) and plasmid replicons. Complete genomes were obtained for the ST1193 isolates DETEC-P836 from a P23 rectal swab, DETEC-E1005 from the BU3 sink, and DETEC-E1070 from the BU11 sink. All three genomes contain the same plasmids, pDETEC3 and pDETEC4.

Other examples of closely related isolates from different patients or ICU environments include an ST5416 isolated in week 12 from a P23 oral swab. This ST had been isolated previously from P2 in bed unit 6, in week 9, which was the same week P23 was admitted to the ICU. The ST5416 isolates differed by 1 SNP and contained the same ARGs and plasmid replicons. ST167 isolates with 0 SNPs were found 7 weeks apart, from the bed curtain of BU9 in week 2 and from the sink overflow of BU1 in week 9, associated with P8 and P9, respectively (Fig. 2B). P8 had occupied BU9 in week 2, at which point they were adjacent to P9, who was in BU10 from week 2 to week 4. After a 4-week absence from the ICU, P9 was in BU1 when ST167 was isolated from its sink overflow. ST174 isolates that differed by 1 SNP were obtained from rectal swabs from two different staff members, but they carried different *bla*$_{CTX-M}$ genes. ST393 isolates from a staff rectal swab and a clinical specimen from 2020 that carried *bla*$_{CTX-M-27}$ had identical genomes (0 SNPs). They appeared to represent the only ESBL-EC strain found in both the clinical and ICU surveillance collections.

Diverse ESBL resistance determinants were found in diverse genetic contexts. CTX-M-type β-lactamases were the dominant ESBL resistance determinants in this collection, with one or more *bla*$_{CTX-M}$ genes found in 159 of the 165 isolates (96.4%). Most isolates (143/159, 89.9%) contained a single *bla*$_{CTX-M}$ gene, while 16 contained two different *bla*$_{CTX-M}$ genes (Fig. 1). The *bla*$_{CTX-M-55}$ gene was the most common in the collection (67 isolates, 27 STs), followed by *bla*$_{CTX-M-14}$ (41 isolates, 15 STs), *bla*$_{CTX-M-15}$ (23 isolates, 7 STs), *bla*$_{CTX-M-65}$ (22 isolates, 11 STs), *bla*$_{CTX-M-27}$ (15 isolates, 7 STs), *bla*$_{CTX-M-3}$ (2 isolates, both ST1193), and *bla*$_{CTX-M-24}$ (1 isolate, ST69). Amongst the isolates that carried two *bla*$_{CTX-M}$ genes, nine had *bla*$_{CTX-M-55}$ with *bla*$_{CTX-M-65}$, six had *bla*$_{CTX-M-55}$ with *bla*$_{CTX-M-14}$, and one had *bla*$_{CTX-M-15}$ with *bla*$_{CTX-M-14}$. Of the six isolates that lacked *bla*$_{CTX-M}$ genes, three ST167 isolates carried *bla*$_{CMY-146}$, a ST457 isolate carried *bla*$_{CMY-2}$, a ST706 isolate carried *bla*$_{DHA-1}$, and a ST453 isolate carried only *bla*$_{TEM}$ (Fig. 1).

We determined the context of *bla*$_{CTX-M}$ genes in 93 of the 165 isolates in the collection, by examining complete genomes (23 isolates) or *bla*$_{CTX-M}$-containing contigs in draft genomes (70 isolates). In the remaining cases, *bla*$_{CTX-M}$ genes were found in contigs that included only mobile element sequences and therefore did not contain sufficient information to reliably determine their locations. Of the 93 instances where the locations of *bla*$_{CTX-M}$ genes were determined, 44 were in chromosomes and 50 were in plasmids (one isolate carried copies of *bla*$_{CTX-M-55}$ in its chromosome and in a plasmid). In 55 cases, *bla*$_{CTX-M}$ genes were located in complete IS*Ecp1* TPUs for which boundary sequences could be determined. The sizes of these TPUs ranged from 2,841 bp to 18,201 bp (Table S5).

The 55 complete IS*Ecp1*-*bla*$_{CTX-M}$ TPUs were inserted in 18 different positions in chromosomes and seven in plasmids (Table S5). All complete TPUs were flanked by 5-bp target site duplications (TSDs). Three TPU-insertion position combinations were seen in multiple STs. A 2,845-bp chromosomal unit was flanked by the TSD TGTTT in five ST1236 isolates and one isolate each of ST1485 and 3941. The other combinations found in multiple STs were associated with I-complex plasmids, namely, a 2,971-bp unit in an I1 plasmid was in five STs and a 3,060-bp unit in a Z plasmid was in three STs. This suggested that *bla*$_{CTX-M}$-bearing I1 and Z-type plasmid lineages might be circulating in this *E. coli* population.

I-complex plasmid lineages found in multiple STs. To investigate the possibility that the same I1 and Z plasmid lineages were present in multiple STs in this *E. coli* population, we compared complete plasmid sequences to one another and to contigs from draft genomes that represent incomplete plasmid sequences.

I1 plasmids containing a 2,971-bp IS*Ecp1*-*bla*$_{CTX-M-55}$ TPU flanked by the TSD TACTT were found in six isolates in this collection one ST1011 and two ST1193 isolates from clinical specimens and one isolate each of ST93, ST167, and ST196 from ICU staff rectal swabs. The backbones of these plasmids were typical representatives of the I1 type (Fig. 3A), containing shufflons and complete transfer regions like those of the reference plasmid R64 (10). Based on the presence of two recombinant patches in their backbones, the I1 plasmids in this collection were divided into two sublineages, represented by pDETEC69 and pDETEC73 in Fig. 3A. The plasmids from ST93 and ST167 isolates belonged to the pDETEC69 sublineage, while those from ST196, ST1011, and ST1193 isolates belonged to the pDETEC73 sublineage.

Z plasmids containing a 3,050-bp IS*Ecp1*-*bla*$_{CTX-M-14}$ TPU flanked by the TSD GCGGA were found in four isolates in this collection: a ST131 isolate from a clinical specimen, a ST58 isolate from an ICU patient rectal swab, and ST95 and ST131 isolates from ICU staff rectal swabs. Similar to the situation seen amongst I1 plasmids, the Z plasmids could be divided into sublineages on the basis of backbone recombination patches. Plasmids from the patient ST58 (pDETEC82) and staff ST131 (pDETEC79) isolates belonged to the same sublineage. Apart from rearrangements in the shufflon region (which was also interrupted by IS*1* in pDETEC82), pDETEC79 and pDETEC82 were almost identical (99.98% nucleotide identity across the 85,765 bp compared).

Both of the signature TPU-backbone junction sequences from the I1 and Z plasmids described above were found in multiple plasmids in GenBank, indicating that these lineages are present in wider enterobacterial populations. Plasmids bearing the I1 plasmid TACTT-flanked IS*Ecp1*-*bla*$_{CTX-M-55}$ insertion ($n = 25$) have been seen in *E. coli*, *Shigella sonnei*, *Salmonella enterica* serovar Typhimurium, *Klebsiella pneumoniae*, and *Enterobacter hormachei* that were isolated from human feces, clinical isolates, animals, and wastewater in China ($n = 18$), Japan ($n = 3$), Kazakhstan, Belgium, Switzerland, and the United Kingdom ($n = 1$ each) (see Table S8 in the supplemental material). Plasmids containing the Z-plasmid GCGGA-flanked IS*Ecp1*-*bla*$_{CTX-M-14}$ insertion ($n = 44$) have been carried by *E. coli*, *K. pneumoniae*, *Salmonella*, and *Shigella* isolated from multiple countries in Asia and Europe, as well as in Australia and the United States (see Table S9 in the supplemental material).

Evidence for *bla*$_{CTX-M}$ transmission from specific plasmid lineages to chromosomes. To investigate the dynamics of their interhost and intermolecular transmission, we examined the contents of complete chromosomal IS*Ecp1*-*bla*$_{CTX-M-55}$ TPUs. In six cases, we were able to definitively identify the plasmid lineages that chromosomal insertions were derived from. In the ST131 isolate DETEC-S573 from an ICU staff rectal swab, *bla*$_{CTX-M-55}$ is located in a 6,397-bp IS*Ecp1* TPU inserted in the chromosome and flanked by the TSD TTGAT (Fig. 3B). The 6,397-bp TPU includes 3,426 bp of the I1 plasmid backbone from immediately adjacent to the 2,971-bp TPU described above, including one copy of the associated TSD sequence TACTT. Thus, we conclude that the 6,397 bp TPU in this ST131 chromosome is derived from the I1 plasmid lineage present in multiple STs in this ESBL-EC population (Fig. 3B). As DETEC-S573 does not contain an I1 plasmid, the plasmid must have been lost after delivering the *bla*$_{CTX-M-55}$ gene.
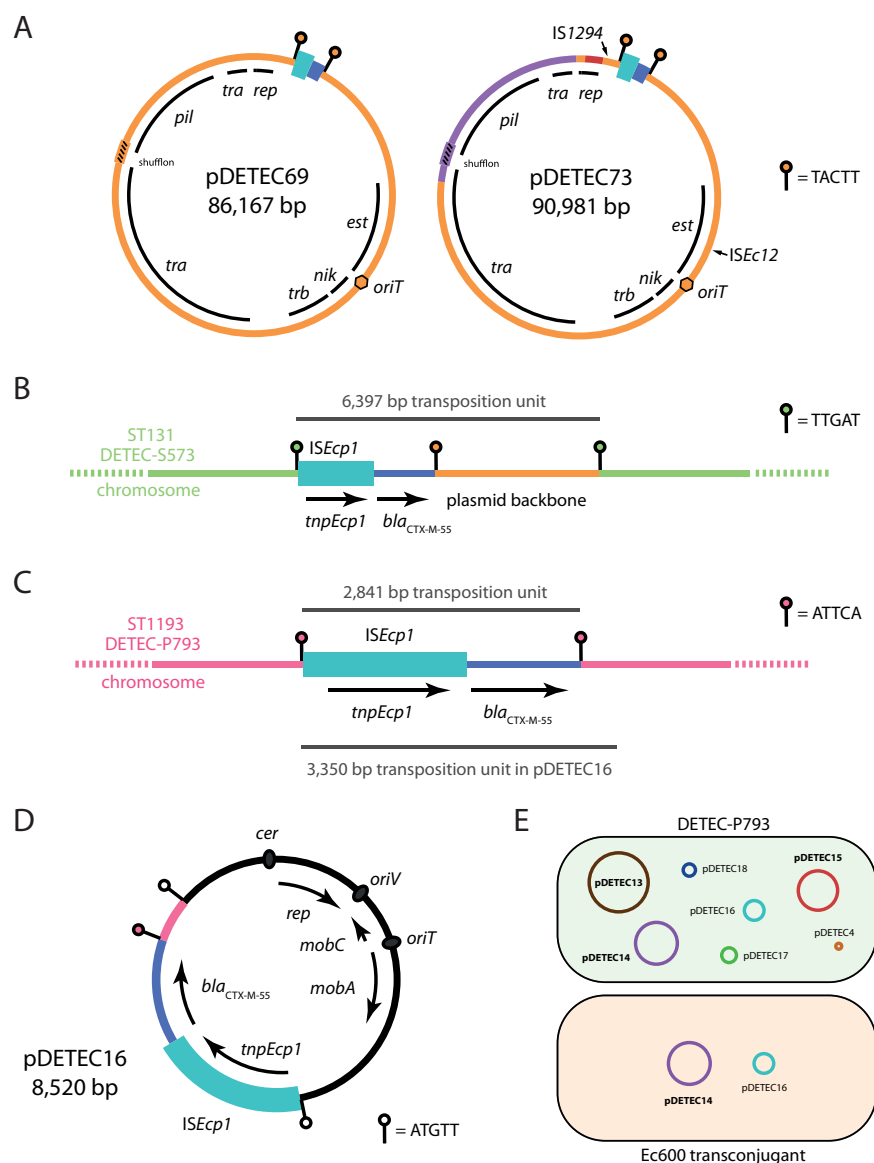
FIG 3 Plasmids, transposition units, and bla_{CTX-M} movement. (A) Circular maps of the I1 plasmids pDETEC69 and pDETEC73. The extents of replication (*rep*), transfer (*tra* and *trb*), thin pilus biogenesis (*pil*) and establishment (*est*) regions are shown. IS*Ecp1*-bla_{CTX-M} TPUs are shown as cyan/blue boxes flanked by lollipops that indicate the position and sequence of target site duplications. Purple and maroon segments in pDETEC73 represent recombinant sequences. (B) IS*Ecp1*-$bla_{CTX-M-55}$ TPU in the chromosome of ST131 isolate DETEC-S573. (C) IS*Ecp1*-$bla_{CTX-M-55}$ TPU in the chromosome of ST1193 isolate DETEC-P793. (D) Small $bla_{CTX-M-55}$-bearing plasmid pDETEC16. (**E**) Co-transfer of pDETEC16 and pDETEC14. Shaded cells represent DETEC-P793 and a transconjugant derived from mating DETEC-P793 with *E. coli* Ec600. The plasmids in each host are shown as labeled circles. A to D of this figure are drawn to different scales, but IS*Ecp1* (1,656 bp) is shown in each, and the sizes of TPUs in B and C are indicated.

Similarly, we determined that a further five H-type, F-type, and I-complex plasmid lineages were the sources of other chromosomal TPUs in the collection (Table 1).

Transposition and mobilization of $bla_{CTX-M-55}$ from a ST1193 chromosome. The complete genome of ST1193 patient rectal isolate DETEC-P793 contained two copies of $bla_{CTX-M-55}$, one in the chromosome and one in a small plasmid. The chromosomal copy is in a 2,841-bp IS*Ecp1* TPU (Fig. 3C). The second copy is in the 8,520-bp plasmid pDETEC16 (Fig. 3D). The IS*Ecp1*-$bla_{CTX-M-55}$ TPU in pDETEC16 is 3,350 bp and flanked by the 5-bp target site duplication ATGTT (Fig. 3D). The final 509 bp of the TPU is identical to the sequence adjacent to the DETEC-P793 chromosomal TPU (Fig. 3D). This finding

TABLE 1 Plasmid-derived chromosomal IS*Ecp1-bla*$_{CTX-M}$ transposition units in this collection

Gene	TPU size (bp)	Host ST	Source plasmid lineage information	
			Replicon type	Representative plasmid[a]
bla$_{CTX-M-14}$	3,445	354	I-complex[b]	
	4,477	38	FII-2	HM355591
bla$_{CTX-M-55}$	3,050	12742	HI2	AP023198
	5,800	617	I2	LR890295
	6,397	131	I1	CP116096
bla$_{CTX-M-64}$	18,201	48	HI2	MT773678

[a]GenBank accession no.
[b]A representative of this lineage was not present in GenBank, so its replicon type could not be determined. However, the plasmid backbone sequence in this TPU is identical to part of the backbone of Z-type plasmid pDETEC33 (GenBank accession no. CP116125), which does not contain *bla*$_{CTX-M-14}$.

indicates that the TPU in pDETEC16 was acquired from its host's chromosome. pDETEC16 has a ColE2-like backbone that contains a putative origin-of-transfer (*oriT*) and MOB$_{Q4}$-type mobilization determinants (Fig. 3D).

Three of the seven plasmids carried by DETEC-P793 contain complete transfer regions (Fig. 3E). We mated DETEC-P793 with *E. coli* Ec600 in order to determine whether any of the large plasmids in DETEC-P793 could mobilize pDETEC16. Transconjugants were obtained at a mean frequency of 8.55×10^{-6} per donor. Five transconjugants were screened for the presence of pDETEC16 and all three putative conjugative plasmids by PCR. The I1 plasmid pDETEC14 was detected along with pDETEC16 in all transconjugants, while pDETEC13 and pDETEC15 were not detected in any transconjugants (Fig. 3E). This demonstrated that pDETEC14 had mobilized pDETEC16 in the laboratory. Mobilization of pDETEC16 by an I1 plasmid is consistent with previous studies that have shown that MOB$_{Q4}$-type plasmids can be mobilized by I-complex plasmids (11).

**Carbapenem resistance associated with IS*1*-mediated amplification of *bla*$_{CMY-146}$.** All isolates were tested for susceptibility to meropenem, and just four isolates exhibited resistance. Carbapenem resistance in the ST410 clinical isolate DETEC-C6 and the ST48 patient rectal swab isolate DETEC-P61 could be explained by the presence of the *bla*$_{NDM-5}$ metallo-β-lactamase gene. The two remaining meropenem-resistant isolates were ST167 and contained *bla*$_{CMY-146}$, which is not expected to confer resistance to carbapenems. DETEC-P351 was isolated from a P11 rectal swab in week 3 and DETEC-E471 from P11's bed unit environment a week later (Fig. 2). The complete genome of DETEC-P351 contains seven copies of *bla*$_{CMY-146}$. Six copies are in the 77,960-bp I1 plasmid pDETEC6, and the seventh copy is in the chromosome (Fig. 4A). The copies of *bla*$_{CMY-146}$ in pDETEC6 are interspersed with copies of IS*1*, in a configuration that resembles structures produced by IS*26* (12). Consistent with the amplification of *bla*$_{CMY-146}$ by IS*1* in the I1 plasmid context, we found a putatively ancestral I1 plasmid in GenBank (pECY56; accession KU043116) that contains just a single copy of *bla*$_{CMY}$, with flanking sequences identical to those in pDETEC6 (Fig. 4B).

The chromosomal *bla*$_{CMY-146}$ gene in DETEC-P351 lies between two copies of IS*1* in what appears to be a 4,266-bp compound transposon flanked by the 9-bp TSD GGACCTGCC (Fig. 4A). The 2,730-bp passenger sequence between the copies of IS*1* is identical to the amplified segment in pDETEC6. The chromosomal copy of *bla*$_{CMY-146}$ is therefore likely to have been acquired from pDETEC6.

Internationally distributed multidrug resistance plasmid lineages in the ICU. We have generated 91 complete plasmid sequences as part of this study (see Table S10 in the supplemental material). These sequences represent a diverse spectrum of plasmid types, including commonly described large plasmids, phage-plasmids, and small plasmids that utilize rolling-circle replication or theta replication with RNA (θ-RNA) or protein (θ-Rep) initiators. Forty of the complete plasmids contain one or more antibiotic resistance genes. Most ARG-containing plasmids were F-types ($n = 24$) or I-complex ($n = 10$), with the remainder being X-types ($n = 2$), a phage-plasmid, a H-type plasmid, a θ-RNA plasmid, and a θ-Rep plasmid ($n = 1$ each).

Amongst the F-type plasmids, we found examples of well-characterized internationally distributed lineages. Four complete plasmids contained FII-33 replicons, and when
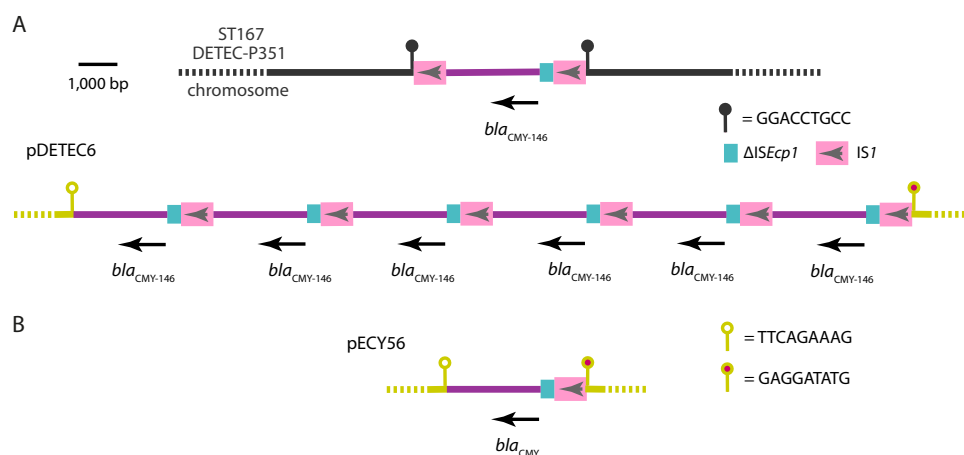
FIG 4 Amplification of $bla_{CMY-146}$ in *E. coli* ST167. Scaled diagrams showing contexts of $bla_{CMY-146}$ in DETEC-P351 (A) and the context of bla_{CMY} in pECY56 (B). IS*1* is shown as pink boxes with arrows indicating the orientation of transposase genes. Fragments of IS*Ecp1* are shown as cyan boxes, and the amplified sequence containing bla_{CMY} is shown as purple lines. The DETEC-P351 chromosome is shown as a black line, and the pDETEC6/pECY56 backbone is shown as a staggered gray line. Lollipop shapes indicate the positions of the sequences shown.

we examined draft genomes, we found FII-33 replicons in a further 22 isolates. We have recently described the diversity and evolution of the FII-33 plasmid lineage, which is endemic in China, internationally disseminated, and strongly associated with multidrug resistance in *E. coli* and *K. pneumoniae* (13). Seven complete plasmids were members of F-type ColV/ColBM lineages that carry colicin and virulence genes (Table S10), and a further 27 draft genomes contain all or part of the *cvaC* colicin V gene. The virulence-associated genes in ColV/ColBM plasmids include those for siderophores, such as aerobactin and salmochelin, which are thought to contribute to extraintestinal virulence in *E. coli* (14, 15). Acquisition of these plasmids has played an important role in the evolution of some pathogenic *E. coli* lineages, and they have been associated with pandemic lineages, such as ST131, ST95, and ST58 (16, 17). ColV and ColBM plasmid lineages are known to have acquired antibiotic resistance determinants (17), and all five complete examples in this collection contained multiple resistance genes in complex resistance regions.

DISCUSSION

This study has provided a high-resolution 3-month snapshot of ESBL-resistant *E. coli* in an ICU. The bacterial population was diverse, with transient environmental strains related to those isolated from patients, while strains isolated from staff were generally distinct. ESBL resistance determinants were also diverse, and although $bla_{CTX-M-55}$ and $bla_{CTX-M-14}$ dominated, they were found in various contexts in plasmids and chromosomes. Some bla_{CTX-M}-bearing plasmid lineages were found across the disparate *E. coli* populations or were shown to have introduced bla_{CTX-M} genes that transposed into host chromosomes as passengers in IS*Ecp1* TPUs. Our close examination of IS*Ecp1* TPUs also allowed us to detect the movement of $bla_{CTX-M-55}$ from a chromosomal site to a mobilizable plasmid in a ST1193 strain (Fig. 3C to E).

There was a strong relationship between isolates found in ICU patients and those found in their bed unit environments. However, we observed limited strain persistence in the ICU environment. Although instances of highly similar isolates being found in multiple bed unit environments were rare, we observed more of them in the six-bed room (BU9-12; ST744, ST131, and ST1193) than in other rooms (Fig. 2). This result suggests that ESBL-EC transmission is more likely to occur in multibed ICU rooms. Of the three instances where highly similar isolates were found in bed units in different rooms, two (involving ST1193 and ST167) were associated with sinks. Hospital sinks have been shown in other studies to be important reservoirs of antibiotic-resistant pathogens (18, 19) and to contribute to transmission via plumbing in model systems (20).

Although there was little crossover at strain level between the ICU and clinical collections, some $bla_{\text{CTX-M}}$-bearing plasmid lineages were represented in both, as well as in multiple STs within the ICU surveillance collection. I-complex plasmids (I1 and Z types) were particularly prominent here. The association of $bla_{\text{CTX-M}}$ genes with I-complex plasmids has been noted, and the existence of multiple internationally disseminated lineages (21) suggests that the confluence of these elements has proven successful on many occasions. However, where and under which conditions these and other plasmids are transferring in bacterial populations remain open questions. We did not find evidence for the horizontal transfer of plasmids in this ICU, through our examination of only a single ESBL-EC colony per sample precluded this. A study performed over a 2-year period in a European hospital found evidence for widespread transmission of a single carbapenemase-encoding plasmid, particularly in the gastrointestinal tracts of patients (22).

The diversity of the ICU ESBL-EC population, and its strong association with patient or staff carriage, appears to suggest that new ESBL-EC strains are introduced to the ICU regularly. The 46.3% ESBL-EC carriage rate observed in staff here is indicative of a high community carriage rate, as the ICU staff are healthy adults residing in Guangzhou. Few studies have examined the prevalence of ESBL-EC carriage in healthy Chinese cohorts, and we are not aware of any studies conducted in Guangdong Province. However, studies focusing on healthy adults in Shandong (2013 to 2014) and Shanghai (2014), and children in Hunan (2021) have reported carriage rates of 65.0%, 30.5%, and 35.8%, respectively (23–25). These data highlight the importance of genomic studies targeting community commensal *E. coli* populations (26), which might reveal links to the strains and plasmids that are ultimately associated with hospital infections.

A concerning finding here was the presence of multiple copies of $bla_{\text{CMY-146}}$ in a carbapenem-resistant ST167 strain that lacked carbapenemase genes (Fig. 4). This result appears to be another example where IS-mediated amplification of a β-lactam (27–29) or aminoglycoside (30) resistance gene has yielded an unexpected phenotype. In previous cases, IS*26* has been involved in gene amplification, but here, IS*1* was implicated. As IS*1* is not part of the IS*26* family of elements, for which the study of transposition mechanisms has provided an explanation for observed structures (31), similar molecular examinations of IS*1* transposition are required. More generally, the modulation of clinically relevant β-lactam resistance phenotypes by IS-mediated gene duplications requires further investigation.

Conclusions. The patients, staff, and environment of this ICU hosted a diverse ESBL-EC population over our 3-month study period. Our data suggest that strains are being introduced to the ICU regularly, likely in association with patients, but that these strains do not persist for extensive periods in ICU environments. Plasmid and IS*Ecp1*-mediated transmission of $bla_{\text{CTX-M}}$ genes play major roles in the ongoing spread of ESBL resistance in *E. coli* populations that can enter hospitals.

MATERIALS AND METHODS

Ethics. This study was approved by the Medical Ethics Committee of the First Affiliated Hospital of Guangzhou Medical University on 21 May 2018.

Study design and sampling regimen. This study was conducted in the Internal Medicine ICU of a tertiary care hospital in Guangzhou, China. Sampling occurred weekly over a 13-week period between July and October 2019. Environmental samples were collected from eight single-bed rooms, a six-bed room, and common areas between rooms. A complete list of environmental sampling sites can be found in Table S1 in the supplemental material. Oral and rectal swabs were obtained from each patient present in the ward on each weekly sampling occasion. Staff rectal and coat swabs were collected on three dates over the course of the study. Swabbing was performed with Copan swabs moistened with Mueller-Hinton broth (Shanghai Comagal Microbial Technology Co., Shanghai, China). Environmental sites were swabbed for 1 min and transported to the laboratory at room temperature for culturing. Clinical isolates obtained between September and October 2020 were provided by the hospital's clinical laboratory.

Bacterial isolation and antibiotic susceptibility testing. Swabs were incubated, shaking, at 37℃ in 4 mL of Mueller-Hinton broth until turbidity was observed (usually 16 to 18 h, maximum 24 h). Turbid cultures (50 μL) were spread on CHROMagar ESBL plates (Shanghai Comagal Microbial Technology Co., Shanghai, China) and incubated overnight at 37℃. Presumptive *E. coli* colonies were streaked onto antibiotic-free Mueller-Hinton agar plates (Huankai Microbial Company, Guangzhou, China) and incubated overnight at 37℃. Single colonies from Mueller-Hinton plates were collected for storage at −80℃, further characterization, and

whole-genome sequencing. To determine the proportion of ESBL-EC isolates that were also carbapenem resistant, sensitivity to imipenem and meropenem was assessed by broth microdilution according to CLSI guidelines (M100-S26). *E. coli* ATCC 25922 was used as a quality-control strain.

Plasmid transfer assays. Transfer of the $bla_{CTX-M-55}$-bearing plasmid pDETEC16 was assessed by mating host *E. coli* DETEC-P793 with rifampicin-resistant *E. coli* Ec600. DETEC-P793 and Ec600 overnight cultures (100 μL each) were spread onto the same Mueller-Hinton agar plate and incubated at 37°C overnight. The resulting lawn was harvested and serially diluted in 0.9% sterile saline. Dilutions were plated onto Mueller-Hinton agar containing 20 μg/mL cefepime to select for DETEC-P793, 500 μg/mL rifampicin to select for Ec600, or 20 μg/mL cefepime + 500 μg/mL rifampicin to select for pDETEC16-containing Ec600 transconjugants. Transconjugants were screened for the presence of pDETEC16 and the putative conjugative plasmids pDETEC13, pDETEC14, and pDETEC15 by PCR. Primers and PCR conditions are listed in Table S2 in the supplemental material (32, 33).

Whole-genome sequencing and analysis. Genomic DNA was extracted using a minikit (Qiagen, Hilden, Germany) in accordance with the manufacturer's instructions. Whole-genome sequencing was performed using both the HiSeq (Illumina, San Diego, USA) and the Oxford Nanopore GridION (Nanopore, Oxford, UK) platforms (Tianke, Zhejiang, China).

Illumina sequence reads (2 × 150 bp, paired end) were trimmed and assembled with Shovill v1.1.0 under default settings with a 10× minimum contig coverage (https://github.com/tseemann/shovill). Read quality was determined with FastQC v0.11.8,1, and assemblies were assessed for contamination and completeness using QUAST v5.0.2, CheckM v1.0.13, and ARIBA v2.14.1 with the "*Escherichia coli*" MLST database. All genomes met the following quality expectations: total genome size, 4,580,428 to 5,537,816 bp; N_{50} value of ≥65,734; and GC content of 50.23 to 50.93%.

For hybrid assemblies, Nanopore reads were trimmed with Filtlong v0.2.0 (https://github.com/rrwick/Filtlong) under default settings targeting approximately 100-fold genome coverage. They were assembled with the trimmed Illumina reads using Unicycler v0.4.8 (34) under default settings. For genomes that did not assemble contiguously in this way, Flye v2.7-b1585 (35) was used to assemble long reads first. The resulting Nanopore-only assemblies were input into Unicycler along with short reads under default settings or using bold mode where specified (see Table S3 in the supplemental material). Manual approaches were used to complete some small plasmid assemblies in Gene Construction Kit v4.5.1 (Textco Biosoftware, Raleigh, USA); see Table S3 for details.

Genome characterization. Genomes were initially characterized by using abricate (v0.8.13) to screen with the NCBI AMRFinderPlus and PlasmidFinder databases (both updated 22 September 2021) (36, 37). F-type plasmid replicons were subtyped using the PubMLST database (https://pubmlst.org/organisms/plasmid-mlst).

Phylogenetic analysis was undertaken for all isolates together and separately for each ST with more than three isolates. Reference genomes are listed in Table S4 in the supplemental material. Reference genomes were annotated with Prokka 1.14.0 (38) under default settings. Using Snippy v4.4.5 (https://github.com/tseemann/snippy), isolates from the whole data set and from each ST were aligned against their appropriate reference genome and a multiple sequence alignment was generated for each. When more than three isolates were represented in each alignment, recombination was removed using gubbins v2.4.0 (39) with the FastTree tree builder (40). SNP distances were calculated from resulting recombination-free alignments with SNP-dists v0.6.3 (https://github.com/tseemann/snp-dists). Phylogenetic trees were constructed with FastTree v2.1.10 using the nucleotide alignment setting and a general time reversible model (40).

Plasmid and translocatable element characterization. Gene Construction Kit v4.5.1 (Textco Biosoftware, Raleigh, USA) was used to examine and manually annotate plasmid and other mobile DNA sequences. Plasmid sequences were compared using the standalone and Web-based BLASTn database (41). IS*Ecp1* TPUs were defined by comparison to uninterrupted sequences in the GenBank nonredundant nucleotide database. As IS*Ecp1* represents the "left" end of complete TPUs, the sequence adjacent to it was used to determine each TPU's context and insertion position. A comparison with uninterrupted GenBank sequences facilitated the identification of the "right" ends of TPUs. The extents of TPUs were confirmed by the presence of flanking target site duplications immediately adjacent to their boundaries. To identify plasmids in GenBank that contained specific TPU insertions, the nonredundant nucleotide database was queried with 100-bp sequences that spanned the junctions between TPUs and their adjacent sequences, comprised of 50 bp each from the TPU and the adjacent sequence.

Data availability. Sequencing reads and draft or complete genome sequences are available under NCBI BioProject accession PRJNA907549. Accession numbers for complete plasmid sequences are listed in Table S10.

SUPPLEMENTAL MATERIAL

Supplemental material is available online only.
SUPPLEMENTAL FILE 1, PDF file, 0.5 MB.

REFERENCES

1. Cummins EA, Snaith AE, McNally A, Hall RJ. 2021. The role of potentiating mutations in the evolution of pandemic *Escherichia coli* clones. Eur J Clin Microbiol Infect Dis https://doi.org/10.1007/s10096-021-04359-3.

2. Bevan ER, Jones AM, Hawkey PM. 2017. Global epidemiology of CTX-M β-lactamases: temporal and geographical shifts in genotype. J Antimicrob Chemother 72:2145–2155. https://doi.org/10.1093/jac/dkx146.

3. Xia S, Fan X, Huang Z, Xia L, Xiao M, Chen R, Xu Y, Zhuo C. 2014. Dominance of CTX-M-type extended-spectrum β-lactamase (ESBL)-producing *Escherichia coli* isolated from patients with community-onset and hospital-onset infection in China. PLoS One 9:e100707. https://doi.org/10.1371/journal.pone.0100707.

4. Zeng S, Luo J, Li X, Zhuo C, Wu A, Chen X, Huang L. 2021. Molecular epidemiology and characteristics of CTX-M-55 extended-spectrum β-lactamase-producing *Escherichia coli* from Guangzhou, China. Front Microbiol 12:730012. https://doi.org/10.3389/fmicb.2021.730012.

5. Partridge SR, Kwong SM, Firth N, Jensen SO. 2018. Mobile genetic elements associated with antimicrobial resistance. Clin Microbiol Rev 31:e00088-17. https://doi.org/10.1128/CMR.00088-17.

6. Poirel L, Lartigue M-F, Decousser J-W, Nordmann P. 2005. IS*Ecp1B*-mediated transposition of *bla*$_{CTX-M}$ in *Escherichia coli*. Antimicrob Agents Chemother 49:447–450. https://doi.org/10.1128/AAC.49.1.447-450.2005.

7. Souverein D, Euser SM, Herpers BL, Kluytmans J, Rossen JWA, Den Boer JW. 2019. Association between rectal colonization with highly resistant Gram-negative rods (HR-GNRs) and subsequent infection with HR-GNRs in clinical patients: a one year historical cohort study. PLoS One 14:e0211016. https://doi.org/10.1371/journal.pone.0211016.

8. Wyres KL, Hawkey J, Mirčeta M, Judd LM, Wick RR, Gorrie CL, Pratt NF, Garlick JS, Watson KM, Pilcher DV, McGloughlin SA, Abbott IJ, Macesic N, Spelman DW, Jenney AWJ, Holt KE. 2021. Genomic surveillance of antimicrobial resistant bacterial colonisation and infection in intensive care patients. BMC Infect Dis 21:683. https://doi.org/10.1186/s12879-021-06386-z.

9. Wei L, Wu L, Wen H, Feng Y, Zhu S, Liu Y, Tang L, Doughty E, van Schaik W, McNally A, Zong Z. 2021. Spread of carbapenem-resistant *Klebsiella pneumoniae* in an intensive care unit: a whole-genome sequence-based prospective observational study. Microbiol Spectr 9:e0005821. https://doi.org/10.1128/Spectrum.00058-21.

10. Sampei G-I, Furuya N, Tachibana K, Saitou Y, Suzuki T, Mizobuchi K, Komano T. 2010. Complete genome sequence of the incompatibility group I1 plasmid R64. Plasmid 64:92–103. https://doi.org/10.1016/j.plasmid.2010.05.005.

11. Garcillán-Barcia MP, Cuartas-Lanza R, Cuevas A, de la Cruz F. 2019. Cis-acting relaxases guarantee independent mobilization of MOB$_{Q4}$ plasmids. Front Microbiol 10:2557. https://doi.org/10.3389/fmicb.2019.02557.

12. Harmer CJ, Moran RA, Hall RM. 2014. Movement of IS*26*-associated antibiotic resistance genes occurs via a translocatable unit that includes a single IS*26* and preferentially inserts adjacent to another IS*26*. mBio 5:e01801-14. https://doi.org/10.1128/mBio.01801-14.

13. Hu Y, Moran RA, Blackwell GA, McNally A, Zong Z. 2022. Fine-scale reconstruction of the evolution of FII-33 multidrug resistance plasmids enables high-resolution genomic surveillance. mSystems 7:e0083121. https://doi.org/10.1128/msystems.00831-21.

14. Robinson AE, Heffernan JR, Henderson JP. 2018. The iron hand of uropathogenic *Escherichia coli*: the role of transition metal control in virulence. Future Microbiol 13:745–756. https://doi.org/10.2217/fmb-2017-0295.

15. Wiles TJ, Kulesus RR, Mulvey MA. 2008. Origins and virulence mechanisms of uropathogenic *Escherichia coli*. Exp Mol Pathol 85:11–19. https://doi.org/10.1016/j.yexmp.2008.03.007.

16. Reid CJ, Cummins ML, Börjesson S, Brouwer MSM, Hasman H, Hammerum AM, Roer L, Hess S, Berendonk T, Nešporová K, Haenni M, Madec JY, Bethe A, Michael GB, Schink AK, Schwarz S, Dolejska M, Djordjevic SP. 2022. A role for ColV plasmids in the evolution of pathogenic *Escherichia coli* ST58. Nat Commun 13:683. https://doi.org/10.1038/s41467-022-28342-4.

17. Moran RA, Hall RM. 2018. Evolution of regions containing antibiotic resistance genes in FII-2-FIB-1 ColV-Colla virulence plasmids. Microb Drug Resist 24:411–421. https://doi.org/10.1089/mdr.2017.0177.

18. Constantinides B, Chau KK, Quan TP, Rodger G, Andersson MI, Jeffery K, Lipworth S, Gweon HS, Peniket A, Pike G, Millo J, Byukusenge M, Holdaway M, Gibbons C, Mathers AJ, Crook DW, Peto TEA, Walker AS, Stoesser N. 2020. Genomic surveillance of *Escherichia coli* and *Klebsiella* spp. in hospital sink drains and patients. Microb Genom 6:mgen000391. https://doi.org/10.1099/mgen.0.000391.

19. Weingarten RA, Johnson RC, Conlan S, Ramsburg AM, Dekker JP, Lau AF, Khil P, Odom RT, Deming C, Park M, Thomas PJ, NISC Comparative Sequencing Program, Henderson DK, Palmore TN, Segre JA, Frank KM. 2018. Genomic analysis of hospital plumbing reveals diverse reservoir of bacterial plasmids conferring carbapenem resistance. mBio 9:e02011-17. https://doi.org/10.1128/mBio.02011-17.

20. Aranega-Bou P, Ellaby N, Ellington MJ, Moore G. 2021. Migration of *Escherichia coli* and *Klebsiella pneumoniae* carbapenemase (KPC)-producing *Enterobacter cloacae* through wastewater pipework and establishment in hospital sink waste traps in a laboratory model system. Microorganisms 9:1868. https://doi.org/10.3390/microorganisms9091868.

21. Zong Z, Ginn AN, Dobiasova H, Iredell JR, Partridge SR. 2015. Different IncI1 plasmids from *Escherichia coli* carry IS*Ecp1-bla*$_{CTX-M-15}$ associated with different Tn*2*-derived elements. Plasmid 80:118–126. https://doi.org/10.1016/j.plasmid.2015.04.007.

22. León-Sampedro R, DelaFuente J, Díaz-Agero C, Crellen T, Musicha P, Rodríguez-Beltrán J, de la Vega C, Hernández-García M, R-GNOSIS WP5 Study Group, López-Fresneña N, Ruiz-Garbajosa P, Cantón R, Cooper BS, San Millán Á. 2021. Pervasive transmission of a carbapenem resistance plasmid in the gut microbiota of hospitalized patients. Nat Microbiol 6:606–616. https://doi.org/10.1038/s41564-021-00879-y.

23. Ni Q, Tian Y, Zhang L, Jiang C, Dong D, Li Z, Mao E, Peng Y. 2016. Prevalence and quinolone resistance of fecal carriage of extended-spectrum β-lactamase-producing *Escherichia coli* in six communities and two physical examination center populations in Shanghai, China. Diagn Microbiol Infect Dis 86:428–433. https://doi.org/10.1016/j.diagmicrobio.2016.07.010.

24. Zhang H, Zhou Y, Guo S, Chang W. 2015. High prevalence and risk factors of fecal carriage of CTX-M type extended-spectrum beta-lactamase-producing Enterobacteriaceae from healthy rural residents of Taian, China. Front Microbiol 6:239. https://doi.org/10.3389/fmicb.2015.00239.

25. Liu X, Li X, Yang A-W, Tang B, Jian ZJ, Zhong YM, Li HL, Li YM, Yan Q, Liang XH, Liu WE. 2022. Community fecal carriage and molecular epidemiology of extended-spectrum β-lactamase- and carbapenemase-producing *Escherichia coli* from healthy children in the Central South China. Infect Drug Resist 15:1601–1611. https://doi.org/10.2147/IDR.S357090.

26. Marin J, Clermont O, Royer G, Mercier-Darty M, Decousser JW, Tenaillon O, Denamur E, Blanquart F. 2022. The population genomics of increased virulence and antibiotic resistance in human commensal *Escherichia coli* over 30 years in France. Appl Environ Microbiol 88:e0066422. https://doi.org/10.1128/aem.00664-22.

27. Hubbard ATM, Mason J, Roberts P, Parry CM, Corless C, van Aartsen J, Howard A, Bulgasim I, Fraser AJ, Adams ER, Roberts AP, Edwards T. 2020. Piperacillin/tazobactam resistance in a clinical isolate of *Escherichia coli* due to IS*26*-mediated amplification of *bla*$_{TEM-1B}$. Nat Commun 11:4915. https://doi.org/10.1038/s41467-020-18668-2.

28. Hansen KH, Andreasen MR, Pedersen MS, Westh H, Jelsbak L, Schønning K. 2019. Resistance to piperacillin/tazobactam in *Escherichia coli* resulting from extensive IS*26*-associated gene amplification of *bla*$_{TEM-1}$. J Antimicrob Chemother 74:3179–3183. https://doi.org/10.1093/jac/dkz349.

29. Bontron S, Poirel L, Kieffer N, Savov E, Trifonova A, Todorova I, Kueffer G, Nordmann P. 2019. Increased resistance to carbapenems in *Proteus mirabilis* mediated by amplification of the *bla*$_{VIM-1}$-carrying and IS*26*-associated class 1 integron. Microb Drug Resist 25:663–667. https://doi.org/10.1089/mdr.2018.0365.

30. Harmer CJ, Lebreton F, Stam J, McGann PT, Hall RM. 2022. Mechanisms of IS*26*-mediated amplification of the *aphA1* gene leading to tobramycin resistance in an *Acinetobacter baumannii* isolate. Microbiol Spectr 10:e0228722. https://doi.org/10.1128/spectrum.02287-22.

31. Harmer CJ, Hall RM. 2019. An analysis of the IS*6*/IS*26* family of insertion sequences: is it a single family? Microb Genom 5:e000291. https://doi.org/10.1099/mgen.0.000291.

32. Moran RA, Anantham S, Pinyon JL, Hall RM. 2015. Plasmids in antibiotic susceptible and antibiotic resistant commensal *Escherichia coli* from healthy Australian adults. Plasmid 80:24–31. https://doi.org/10.1016/j.plasmid.2015.03.005.

33. Carattoli A, Bertini A, Villa L, Falbo V, Hopkins KL, Threlfall EJ. 2005. Identification of plasmids by PCR-based replicon typing. J Microbiol Methods 63:219–228. https://doi.org/10.1016/j.mimet.2005.03.018.

34. Wick RR, Judd LM, Gorrie CL, Holt KE. 2017. Unicycler: resolving bacterial genome assemblies from short and long sequencing reads. PLoS Comput Biol 13:e1005595. https://doi.org/10.1371/journal.pcbi.1005595.

35. Kolmogorov M, Yuan J, Lin Y, Pevzner PA. 2019. Assembly of long, error-prone reads using repeat graphs. Nat Biotechnol 37:540–546. https://doi.org/10.1038/s41587-019-0072-8.

36. Feldgarden M, Brover V, Haft DH, Prasad AB, Slotta DJ, Tolstoy I, Tyson GH, Zhao S, Hsu CH, McDermott PF, Tadesse DA, Morales C, Simmons M,

Tillman G, Wasilenko J, Folster JP, Klimke W. 2019. Validating the AMR-Finder tool and resistance gene database by using antimicrobial resistance genotype-phenotype correlations in a collection of isolates. Antimicrob Agents Chemother 63:e00483-19. https://doi.org/10.1128/AAC.00483-19.

37. Carattoli A, Zankari E, García-Fernández A, Voldby Larsen M, Lund O, Villa L, Møller Aarestrup F, Hasman H. 2014. In silico detection and typing of plasmids using PlasmidFinder and plasmid multilocus sequence typing. Antimicrob Agents Chemother 58:3895–3903. https://doi.org/10.1128/AAC.02412-14.

38. Seemann T. 2014. Prokka: rapid prokaryotic genome annotation. Bioinformatics 30:2068–2069. https://doi.org/10.1093/bioinformatics/btu153.

39. Croucher NJ, Page AJ, Connor TR, Delaney AJ, Keane JA, Bentley SD, Parkhill J, Harris SR. 2015. Rapid phylogenetic analysis of large samples of recombinant bacterial whole genome sequences using Gubbins. Nucleic Acids Res 43:e15. https://doi.org/10.1093/nar/gku1196.

40. Price MN, Dehal PS, Arkin AP. 2009. FastTree: computing large minimum evolution trees with profiles instead of a distance matrix. Mol Biol Evol 26:1641–1650. https://doi.org/10.1093/molbev/msp077.

41. Camacho C, Coulouris G, Avagyan V, Ma N, Papadopoulos J, Bealer K, Madden TL. 2009. BLAST+: architecture and applications. BMC Bioinformatics 10:421. https://doi.org/10.1186/1471-2105-10-421.